International Research Journal of Engineering and Technology (IRJET) e-ISSN: 2395-0056
Volume: 12 Issue: 04 | Apr 2025 www.irjet.net p-ISSN: 2395-0072

A Universal Platform for Multitarget Tracking Radar System Modeling and Analysis with a Performance Comparison of Common Algorithms

Mustafa Latif Çobankaya[1]*, Alaaeldeen Elrouby[2]

[1] *Secretariat of Defence Industries, Ankara, Turkey;*
[2] *Department of Electrical and Electronics Engineering, Ankara Yildirim Beyazit University, Turkey;*

Abstract: Radar system studies are mostly done on the development and optimization of specific components. While investigating and improving specific parts, interactions among the components of radar systems have been receiving less focus. Thus, more wholistic approaches for the modeling and analysis of end-to-end radar system platforms represent valuable contributions to fill in this gap. For this aim, a universal platform for modeling and analyzing end-to-end multitarget tracking (MTT) radar systems is proposed in this study. In the proposed platform, radar system properties, scanning parameter settings, target parameters, and MTT algorithms are configurable in a flexible and seamless manner. The paper also presents a case study which is developed on the platform, providing a performance comparison of three dominant MTT algorithms: Global Nearest Neighbor (GNN), Joint Probabilistic Data Association (JPDA), and Multiple Hypothesis Tracking (MHT). The scenario in the case study comprises MTT of 8 highly maneuvering targets in close proximity. The three algorithms are compared based on their performance and computational complexity levels, measured by the Optimal Sub-Pattern Assignment (OSPA) distance and computational time, respectively. The case study configuration demonstrates the flexibility of the proposed radar system platform for modeling and analyzing MTT radar systems. The results indicate that the JPDA algorithm emerges as the best choice for MTT of highly maneuvering targets in close proximity.

Keywords: Multitarget tracking algorithms; radar system simulation; performance comparison; target motion scenario; OSPA metric

1. Introduction

Radar systems and multitarget tracking (MTT) have been studied for many years that we can find over 100 years of history about radar systems [1], [2]. The classification of radar systems has several approaches such as: according to their base (ground-based, airborne radars), their frequency band (L-band, C-band, millimeter wave radars), antenna type (phased array, AESA radars), or waveform (continuous wave, pulsed radars), and even according to their functionality or mission (weather, fire control, early warning radars) etc. This wide variation is a result of long immense efforts and massive number of research, design, and development studies in this area.

1.1 Wholistic Approach for MTT Radar System Modeling and Analysis

In the literature, most of MTT radar system studies aim at increasing the efficiencies of certain radar system components. They focus on optimizing or finding new solutions for specific parts of radar systems in specific cases. For example, in [3], a dynamic multi-objective particle swarm optimization (DMOPSO) with the assistance of a Kalman filtering prediction strategy was proposed. They increased the performance of antenna deployment for special cases of distributed multi-static radars in multiple surveillance regions in a dynamic environment. DMOPSO method is an optimization of the classical multi-objective particle swarm optimization (MOPSO) method. On the other hand, since during the numerical tests, or after them, the DMOPSO strategy was not tested via a simulation of a comprehensive radar system case, if there is any extra side effect to a certain radar system part, it could not be revealed. In another study, an adaptive beam burden management, named adaptive beam and pulse number scheduling (ABPNS) strategy, was developed to increase the performance of MTT for special situations of distributed radar networks with limited beam resources [4]. On the other hand, constant velocity model was preferred for the targets in the study. Other target model types like constant acceleration or maneuvering targets were not studied and they may have extra unexpected effects on the results. Also, since the simulations were not done on a whole radar system, the effect of ABPNS on other parts of radar system could not be investigated.

Development of a low probability of intercept-based power resource allocation (LPI-PRA) scheme was presented for the application of distributed multiple-input multiple-output (MIMO) dual-function radar communication (DFRC) systems in [5]. They tried to minimize the total power consumption of the overall system by optimizing the transmit power allocation with their approach. On the other hand, the simulations were not done on a complete radar system. Thus,

still there may be an unexpected and unrevealed side effect on another radar component or radar performance. In [6], optimizing the design of transmit beampattern with constant modulus (CM) constraint in Multiple-Input Multiple-Output (MIMO) radar systems was studied to achieve a good trade-off between the performance and the complexity. Together with the superior results to the existing ones, a whole radar system was not operated or simulated during the study. Thus, any bad side effect, if exists, remains unrevealed.

Like the given examples, many more studies focus on the optimization and development of specific parts of the radar systems or become valid for special cases, special radar types and for specific scenarios. On the other hand, in a holistic approach, mutual interactions of subsystems should be also considered, and various conditions and scenarios should be tested for validity.

From this aspect, while specialized studies are valuable for increasing performance of individual components, a comprehensive understanding of how subsystems interact and perform under various conditions is also essential. On the other hand, comprehensive end-to-end (aka holistic) studies on radar systems have received limited focus in the published research literature [7]. Furthermore, most MTT studies are conducted by adding various levels of artificial noise to the motion trajectories of targets, and end-to-end radar system designs are not used during simulations [8]–[12]. Thus, the availability of a comprehensive system model for MTT radar systems would be of a high value for research in the area. Developing such a system model opens the door to explore numerous “what-if?” scenarios and facilitates performance enhancement from the perspectives of MTT algorithms, radar waveforms, signal processing, and optimization. Moreover, it enables the investigation of problems related to the integration of radar system components and provides guidance for their solutions. This study aims to fill that gap by introducing an end-to-end platform for modeling MTT radar systems and presents a case study for its performance assessment. Other targeted features for the proposed platform are flexibility in studying various aspects of MTT radar systems, and its seamlessness in changing the platform parameters and settings.

1.2. MTT Problem and Three Common Algorithms in MTT Applications

The problem of MTT holds significant importance in various military and civilian applications, including air and ground traffic monitoring and control, harbor and underwater surveillance, maritime traffic control and target recognition, oceanography, video communication, military applications, autonomous driving, microbiology, investigating animal lives, satellite systems, electronic warfare, robotics, and various surveillance applications [13]–[17].

Multitarget tracking involves the extraction and estimation of the number of targets, their states, and trajectories from noisy antenna or sensor measurements. As basic examples from daily life, humans perform target detection and tracking while driving a car, walking through streets, during shopping, and when looking for something. The goal of MTT is to estimate the number of targets and their trajectories based on the collected data and accurately associate the data during estimations. In data association, the main question is, “Which measured points correspond to which targets?”. With the wide range of applications for the MTT, different algorithms have been suggested, used, analyzed, and compared in performance and accuracy [18], [19]. Among those algorithms, we believe that the following three algorithms are the dominant in real time applications:

1.2.1. Global Nearest Neighbor

The Global Nearest Neighbor (GNN) algorithm associates each target with the closest measurement in the target space [20]. GNN makes decisions based only on the last measurement value and does not consider any history, meaning it does not use, save, or restore previous estimation values. As a result, any mis-association cannot be corrected. GNN has the lowest computational complexity but is generally considered to have the worst accuracy and performance among MTT algorithms. Nevertheless, it is commonly used in radar applications due to its simplicity where few targets are on the scene [21].

1.2.2. Joint Probabilistic Data Association

The Joint Probabilistic Data Association (JPDA) algorithm calculates the probabilities of targets being at the measured points at each association step. Over time, some probabilities decrease to very small values and are subsequently discarded. The remaining high probabilities undergo the same pruning process at each association step, resulting in weighted sums of all association steps [22]. This method, which incorporates the history of target probabilities, allows JPDA to achieve better accuracy than the GNN algorithm. By this means, JPDA differentiates itself from GNN by maintaining a history of probabilities and making decisions based on that history.

JPDA does not save and store hypotheses but only instantaneous probabilities. The remaining information about hypotheses is solely represented by their probability values. This approach significantly reduces the complexity of the association procedure, while decisions are made using historical values. In contrast, the GNN algorithm associates each target with the closest measurement in the target space disregarding histories of target motions. However, this operation can miss some feasible and potential associations. In this regard, JPDA appears more appealing as it eliminates and discards infeasible hypotheses at each estimation step [23].

1.2.3. Multiple Hypothesis Tracking

The Multiple Hypothesis Tracking (MHT) algorithm is the most complex one among the three algorithms while it is an old one [24]. MHT keeps tracks of all the possible association hypotheses over time. However, the number of association hypotheses grows exponentially, leading to potentially high numbers within a few estimation steps. For example, the number of hypotheses can increase from a single digit to a three-digit number within only three estimation steps during track of a few targets. Therefore, generally additional pruning methods are necessary to reduce computational complexity [19], [25].

When a hypothesis probability value reaches the “track confirmation” region in MHT, it is accepted as the true association result. Conversely, if a hypothesis falls below the threshold of “unlikely track” region, it is pruned away or deleted [26] to prevent the proliferation of hypotheses.

All these MTT algorithms may employ various gating techniques to enhance their performance [27].

1.3. Comparison of the Three Algorithms

Most of the studies in the MTT publications focus on linearly moving targets for comparison and performance evaluation [28], [29]. However, the case study of this paper differs as it focuses on highly maneuvering targets in close proximity to fulfill the needs for more modern and complex scenarios like tracking drones or agile targets. Moreover, this study simulates an end-to-end radar system and uses its data during MTT analysis, providing an additional contribution whereas most simulation studies employ entirely artificial motion data [30].

As a show case for the flexibility and capability of the proposed universal platform, the three MTT algorithms, GNN, JPDA and MHT, are compared based on their performance and computational complexity by applying them on a test case including trajectories of maneuvering targets with multiple close proximity cases. There are some comparison studies for linearly moving or slowly rotating targets in the literature, but comparison of highly maneuvering targets in proximity cases needs to be further investigated.

The contributions of this paper are as follows:

• A universal radar system modeling and simulation platform is proposed and applied on various types of MTT algorithms. This platform offers a holistic approach to radar system investigations, allowing for the analysis of individual components as well as their mutual effects on the overall system performance.

• A comparison study of three dominant MTT algorithms -GNN, JPDA, and MHT- is conducted on a scenario comprising close proximity cases of 8 maneuvering targets. The study presents and discusses estimation results and Optimal Sub-Pattern Assignment (OSPA) values as well as computational complexity results of the MTT algorithms.

In the following sections, the components of the universal radar platform are explained. Section 2 provides detailed explanations of the main sub-blocks of the proposed platform: waveform generation, transmitter and receiver, environment and targets, signal processing, and MTT algorithm. In Section 3, the case study, and its functional structure together with the values of the parameters of the radar components are presented. The results of the case study are analyzed in Section 4. The conclusions are discussed in the final section.

2. The Universal Platform for MTT Radar Systems

The proposed universal platform for MTT radar system represents the end-to-end system, starting from radar waveform generation and extending to the MTT algorithm, with several sub-blocks in between. The platform is developed and implemented in the MATLAB environment.

The proposed platform contains six main sub-blocks: Waveform Generation, Transmitter, Environment & Targets, Receiver, Signal Processing, and MTT Algorithm as illustrated in Figure 1. The radar system scans, detects, and tracks targets within its range for a specified time duration. The sub-blocks of the universal platform with their respective parameters are described in the following subsections.

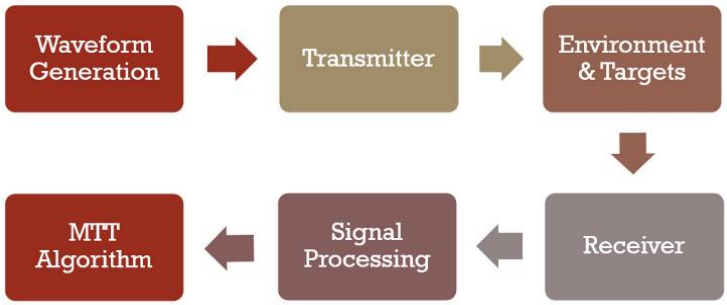

Figure 1. Radar System Sub-Blocks in the Universal Platform

2.1. Waveform Generation

This sub-block is responsible for generating the radar waveform, which can be configured as either an FMCW or pulse waveform, with the possibility of other types as well, depending on the specific needs and applications. The parameters that control the behavior of this sub-block depend on the chosen waveform type.

In pulse radars, the main parameters are peak power, operating frequency, pulse width, and pulse repetition frequency. The latter two parameters play a crucial role in determining the maximum unambiguous range, range resolution and minimum range for the pulsed radar. Peak power affects the radar range whereas the operating frequency has effects on both resolution and range in pulse radars.

In FMCW radars, the key parameters are the operating frequency, sweep time, and sweep bandwidth. The operating frequency is a common parameter, whereas the sweep time and bandwidth are specific to FMCW radars. The sweep time and bandwidth play a crucial role in determining the range, range resolution, and maximum target speed. The frequency modulation can take various forms, such as triangular, sawtooth, sinusoidal, or others. Once the waveform signal is generated, it is transmitted to the transmitter to be launched into the air or any other medium as an electromagnetic wave.

2.2. Transmitter & Receiver

The Tx and Rx sub-blocks represent the output power amplifier and antenna of the transmitter, as well as the low-noise amplifier (LNA) and antenna of the receiver. The parameters that control the behavior of this sub-block are transmitter peak power, transmitter gain, antenna aperture, antenna gain, receiver gain, noise figure, and radar speed.

Transmitter peak power refers to the peak power value of the signal reaching the antenna. The power amplifier amplifies the signal with the value of transmitter gain and sends it to the antenna. The antenna behavior is mainly determined by its gain, bandwidth, radiation pattern, and beamwidth. Additional parameters or features may be included depending on the scenario.

The receiver module amplifies the received signal with its gain value whereas also introducing additional noise indicated by noise figure, resulting in a degradation of the signal-to-noise ratio (SNR). Therefore, the noise figure and receiver gain are two fundamental parameters for the receiver.

Radar speed is added to the platform for scenarios involving airborne radar. In such scenarios, the radar speed is non-zero and influences the behaviors of the transmitter, receiver, and signal processing sub-blocks.

2.3. Environment & Targets

This sub-block determines the parameters and features of the environment and targets. The environment can be free space, water, or any other specific medium. The main factor which environment affects is the power of the received signal and SNR. As a result, the environment has a strong impact on the range of the radar.

The general radar range equation used in the simulation platform is given below:

$$R = \left(\frac{P_t \tau f_r T_i G_t G_r \lambda^2 \sigma}{(4\pi)^3 k T_0 F L (SNR)_0} \right)^{\frac{1}{4}} \quad (1)$$

where, Pt is transmitted peak power, τ is pulse width, fr is pulse repetition frequency (PRF), Ti is the dwell interval in continuous wave radars, Gt and Gr are the transmitter and receiver antenna gain, λ is wavelength, σ is target cross section, k is Boltzman's constant, T0 is the temperature in Kelvin, F is noise figure, L is the total of losses in the system, and (SNR)0 is the minimum SNR required for detection. Ptτfr term is used in pulse radars, and it is replaced with PCW which is average continuous wave (CW) power in CW-based radars. Similarly, Ti denotes the time on target in pulse radars (Mahafza, 2013).

The target types can vary in dimension and include airplanes, UAVs, drones, rockets, warships, submarines, and more, depending on the specific scenario of interest. The primary target parameter of concern is the radar cross section (RCS). The RCS values may vary based on factors such as the target type, dimensions, coatings, directions, and shapes [32], [33].

In the proposed platform, targets are added to the system using a function, named as Add_Targets. This function determines the routes of the targets using the waypointTrajectory function, which is a MATLAB function that builds trajectories based on specified waypoints. By providing positions and corresponding times (e.g., if the target is at location P1 at time T1 and at location P2 at time T2), the waypointTrajectory function generates intermediate locations within the given time intervals.

The position array of targets is constructed using parameters such as the initial and the final times of targets, positions between them, and time increment. The initial time is the time instant of the start of a target's motion. The final time of a target determines the time instant at which its motion ends. The time increment represents the incrementation value of time in the output of the target trajectory building function. Consequently, a smaller time increment results in a higher number of positions along with their corresponding time values in the output.

The final time parameter determines the total active time duration of the radar system. It represents the maximum time up to which targets can have a motion trajectory. If targets exist throughout the entire scan process, they follow their trajectories from the beginning until the final time of the simulation.

2.4. Signal Processing

The signal processing sub-block is developed for scanning and measuring the states of targets, including the detection process. Target detection is done during the scanning process with the scanning parameters which are measurement interval, final time, radar scanning angle, and scan speed.

The measurement interval parameter serves two purposes in the design: it determines the rate of measurement and sets the antenna beamwidth in degrees. For instance, if the measurement interval is set to 10°, measurements are taken at every 10° interval, resulting in an antenna beamwidth of 10° in the azimuth direction. As depicted in Figure 2, the measurement interval equals to the difference between θa and θb, which also represents the antenna beamwidth in the design.

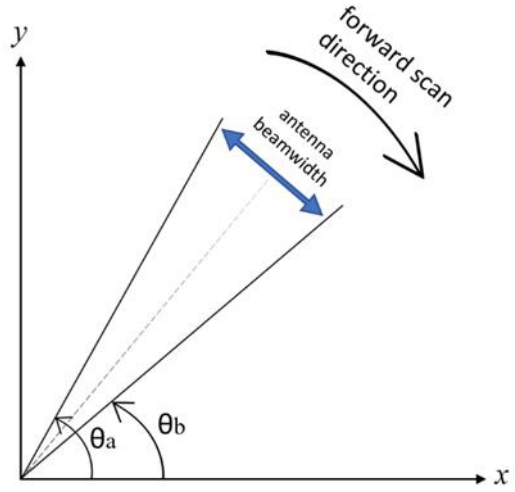

Figure 2. Some Radar Scan Parameters

The radar scanning angle parameter represents the total scanned area of the radar in degrees. Scan speed is the rotation speed of the antenna in rounds per minute. In the platform, the scanning process begins from the y-axis and continues in clockwise direction (forward scanning) until it reaches the specified radar scanning angle. Afterwards, it reverses direction and scans back (counterclockwise) from the final angle until it returns to the y-axis for sectoral scans. For full scan, it starts from y-axis and continues through clockwise direction. Consequently, the forward scan direction is clockwise, starting at the y-axis with 0°, whereas the backward scan follows the opposite direction as shown in FİGURE 2. The platform offers flexibility, allowing for the configuration of alternative scanning approaches.

Using these parameters and their respective values, the platform performs both forward and backward scans, recording measurements in an array. After completion of the scanning process, the array serves as the input data for the MTT algorithm.

2.5. MTT Algorithm

In the developed platform, the MTT sub-block can be configured to implement different algorithms such as GNN, JPDA, MHT, or other algorithms. These three algorithms are preferred in this study since they are the most used ones in real-time studies [34, 35].

In addition to the MTT algorithms, filters should be used to successfully track targets. For filtering, the Kalman Filter and its variants can be used in this sub-block of the platform, including the Extended Kalman Filter (EKF), Unscented Kalman Filter (UKF), and Cubature Kalman Filter (CKF). The Kalman filter (KF) is a powerful recursive algorithm commonly used for estimating the state of a linear dynamic system. It assumes that the system dynamics and measurement model are both linear and that the system noise and measurement noise are Gaussian and additive. However, when dealing with nonlinear motions or nonlinear systems as in our case study, the basic Kalman filter is not appropriate for two basic reasons: Linearity assumption and non-Gaussian noise. The KF relies on the assumption that the system dynamics and measurement model are linear. Thus, the linear approximation used in the KF leads to inaccurate estimates in nonlinear systems. Also, in nonlinear systems or motions, the noise statistics can deviate significantly from Gaussian, making the KF less effective. Non-Gaussian noise can cause the KF to produce biased or suboptimal estimates. As a result, since targets often exhibit nonlinear motion in real-life scenarios, it is preferable to use the EKF, UKF, or CKF in cases involving realistic target motion modeling [36, 37]. Thus, the type of filter is a parameter along with the type and specifications of the MTT algorithm.

Two important parameters for the operation of this sub-block are the confirmation and deletion thresholds of a target. A tentative track is confirmed as a true track when it has at least M1 detections in N1 sequential measurements. Conversely, a tentative track is deleted if it has fewer than M2 detections in N2 sequential measurements. For example, with a confirmation threshold of [3 4], a target is confirmed when it is detected at least M1 = 3 times out of N1 = 4 measurements. Similarly, with a deletion threshold of [5 6], a target is deleted if it disappears at least M2 = 5 times out of N2 = 6 measurements.

Another important parameter is the assignment threshold, which determines the maximum distance at which a measured state can be assigned to a target. In other words, assuming Pn-1 is the position of the target Tm at the step Sn-1, the measured position Pn at the current step Sn is assigned to target Tm only if the distance between Pn and Pn-1 is smaller than the assignment threshold. Targets with distances greater than this threshold cannot be assigned to their respective tracks. In addition, the assignment threshold interacts with the gating technique. Only measurements falling within the gating region are eligible for assignment to the corresponding track.

Number of sensors, maximum number of targets, detection probability, measurement noise, maximum number of tracks, maximum number of sensors are among the other configurable parameters for the MTT algorithm sub-block operation in the proposed platform.

Those mentioned parameters are independent of the type of MTT algorithm, whereas some others are algorithm dependent. For example, maximum number of hypotheses is a parameter in the MHT tracker. It limits the number of hypotheses generated, ensuring that the algorithm does not become overly complex. Consequently, less likely hypotheses are pruned to prevent exceeding the maximum number of hypotheses. Another parameter in MHT is the minimum branch probability. If the probability of a branch drops below the value of it, that branch is pruned. The maximum number of scan history is another special parameter in MHT.

The configuration of an MTT algorithm and its parameters enables the study of a variety of scenarios and facilitates detailed investigation.

3. Case Study: Comparison of the Three Algorithms for MTT of Highly Maneuvering Targets in Proximity

In the case study, a 77 GHz frequency-modulated continuous-wave (FMCW) radar was modeled and simulated for MTT of 8 maneuvering drones within a short range of 600 m and a scanned area of 90° angle. In the MTT sub-block, GNN, JPDA and MHT algorithms were employed for comparison. The motion trajectories of the drones were designed accordingly to ensure close proximity to each other.

The operating frequency was chosen as 77 GHz since it is a free bandwidth in the spectrum suitable for real time developments. Additionally, 77 GHz is widely used in automotive radars [38, 39]. Thus, the universal platform provides compatibility, not only limited to, but also inclusive of research studies in the automotive industry. This proposed design can be utilized in also short-range radar (SRR) network studies [40] and can be suitable for dynamic radar networks of UAVs [41] with additional developments.

The six sub-blocks of the universal radar platform were configured and operated accordingly. Figure 3 shows the functional structure of the FMCW radar system developed on the universal platform for the case study. The names of the functions used are provided in each sub-block, and their duties are explained in the following paragraphs.

Figure 3. Developed FMCW Radar System, Sub-systems and Functions

In the waveform generation sub-block, the "phased.FMCWWaveform" function generates the FMCW signal used in the radar. It takes parameters such as carrier frequency, sweep time, sweep bandwidth, and sweep direction as inputs. The "range2bw" function calculates the required sweep bandwidth, Δf, of the FMCW signal based on the desired range resolution and the speed of signal propagation, which is speed of the light in the case study. Equation (2) describes this below:

$$\Delta f = \frac{c}{2\Delta R} \tag{2}$$

where, c is the speed of light, and ΔR is the range resolution [42].

The "range2beat" function determines the maximum beat frequency, fb, corresponding to the maximum range and the sweep slope as described in (3) below:

$$f_b = \frac{2R_{max}}{c}\frac{\Delta f}{\Delta t} = \frac{2R_{max}}{c} \text{ x } (sweep\ slope) \tag{3}$$

where, Rmax is the maximum range, Δf is the sweep bandwidth and Δt is the sweep time of the generated FMCW signal [31].

In the transmitter sub-block, "aperture2gain" function calculates the antenna gain in dB (G_dB) based on the antenna aperture (A) and the wavelength of the carrier signal (λ), as shown in (4) below [43]:

$$G_{dB} = 10log_{10}(\frac{4\pi A}{\lambda^2}) \quad (4)$$

The "phased.Transmitter" generates the transmitted signal using the parameters of transmitter gain, peak power and loss factor, together with the generated FMCW signal

The environment & targets sub-block includes the "phased.FreeSpace" function, which calculates the signal power attenuation of the transmitted signal in the atmosphere using the general radar equation. The "phased.RadarTarget" simulates the behavior of targets and calculates the effect of the targets on the reflected signal using RCS of them, signal propagation speed and carrier frequency. The "Add_Targets" function determines the ground truth states and their corresponding times for all the targets. It can also generate random motion trajectories if the waypoints are generated randomly. In the motion scenario of the case study, target trajectories are generated in a way that they exhibit maneuvering motion with close proximity to each other.

In the receiver sub-block, the "phased.ReceiverPreamp" function input parameters are receiver gain, loss factor of receiver, noise figure, reference temperature, and sample rate. This function amplifies the received signal. The "phased.Platform" function adds the effect of radar platform motion into the received signal characteristics if the radar has a motion during the scan. By incorporating the platform motion, the function ensures that the received signal accurately represents the real-world scenario and accounts for any changes or disturbances caused by the radar platform's motion.

In the signal processing sub-block, two functions are utilized: "beat2range" and "dop2speed". The "beat2range" function calculates the range of a target by utilizing the beat frequency of the received signal and the sweep slope value. By processing these inputs, the function determines the range or distance between the radar and the target based on the beat frequency observed in the received signal. On the other hand, the "dop2speed" function is responsible for determining the radial speed of a target using the Doppler shift. By analyzing the change in frequency of the received signal caused by the motion of the target relative to the radar, the function calculates the radial velocity of the target. This information is valuable for tracking and analyzing the target's speed. With the help of these functions, the measured positions and radial speeds of targets are extracted in signal processing sub-block.

MTT sub-block estimates the number of targets and their states using MTT algorithm functions "GNN_Tracker", "JPDA_Tracker", "MHT_Tracker", or other similar functions. These three functions were developed specifically for the purpose of performance comparison in this case study. Each tracker function operates independently on the same input, which consists of the measured target states and related times; and conducts the MTT of targets in the scenario separately. Additionally, all the functions utilize the Extended Kalman Filter (EKF) and Interacting Multiple Models (IMM) for filtering. The "OSPA_Metric" function is added to this sub-block for performance evaluations.

The case study was conducted based on this structure of functions, allowing for a comparison of the performance of the three MTT algorithms in the radar system. The FMCW radar system main parameters in the case study and their numerical values are given in Table 1 below:

Table 1. FMCW Radar System Parameter Values

Parameter	Value	Unit
Carrier signal frequency	77	GHz
Sweep time	22	μs
Sweep bandwidth	75	MHz
Sweep direction	up	-
Range resolution	2	m
Signal propagation speed	$3x10^8$	m/s

Range	600	m
Antenna aperture	$3x10^{-4}$	m^2
Transmitter gain	39	dB
Transmitter peak power	3.2	mW
Sample rate	150	MHz
RCS of targets	0.1	m^2
Simulation time	20	s
Number of targets	8	-
Receiver gain	33	dB
Noise figure	4.5	dB
Antenna beamwidth	5	degrees
Scan speed	π	rad/s
Total scanned angle	90	degrees

During waveform generation, an up-sweep linear (sawtooth) FMCW signal was used. FMCW was chosen for its simple architecture and low cost encompassing the expenses associated with the equipment and power consumption. Range resolution was set to 2 m. Consequently, the sweep time of the signal is 18.3 μs, and the sweep bandwidth is found as 75 MHz using (2). Maximum beat frequency is set to 13.64 MHz using (3) and Table 1.

The transmitter in the design has a gain of 39 dB, and the receiver has 33 dB including the antenna gain, which are compatible values with the industry. The receiver noise figure was set to 4.5 dB to be consistent with real-life products and scenarios [44, 45]. The environment is assumed to be free space channel since the radar system is considered as ground-based radar operating in the Earth's atmosphere. The radar RCS of targets is assumed to be 0.1 m^2.

Drones were chosen as targets in this scenario because they are becoming increasingly prevalent in daily life, and there is a growing need for developed radar systems to control, supervise, and regulate their operations in both military and civilian applications. The maximum velocity of the targets is set to 230 km/h which is a high value for drone targets.

In the case study, a sector with 90° angle was scanned in 2-D. Scan speed was chosen as 180°/s, which is applicable in real time scanning. In every single second, a forward scanning and a backward scanning is completed for the scanned area. Thus, during 20 seconds of simulation time, the sector was scanned 40 times in total as formulated in (5):

$$Number\ of\ scans = \frac{scan\ speed \text{ x } simulation\ time}{\text{angle of scanned area}} \tag{5}$$

Error calculations were performed in the case study to evaluate the accuracy of the MTT algorithms. OSPA metric was utilized for error calculations since it is a commonly used metric in performance assessment of MTT algorithms [46-48]. A lower OSPA distance value indicates better tracking performance. OSPA can determine the differences in cardinality and individual elements between two finite sets, which are the true states and estimated states in the case study. The difference in cardinality is found by comparing the number of elements in two sets, whereas the difference in individual elements gives the distance between the corresponding elements of the two sets. For arbitrary finite subsets X={x_1,…,x_m } and Y={y_1,…,y_n }, where m ≤ n, the OSPA distance between X and Y is defined as in (6):

$$\bar{d}_p^{(c)}(X,Y) := \left[\frac{1}{n}\left(\min_{\pi\in\prod_n}\sum_{i=1}^{m} d^{(c)}\left(x_i, y_{\pi(i)}\right)^p + c^p(n-m)\right)\right]^{1/p} \tag{6}$$

where $d^{(c)}(x,y)$ □(:=min(c,d(x,y))) denotes the distance between x, y ∈ W, c (c > 0) is cut off parameter, p (1 ≤ p < ∞) is the order, $\prod_n$ is the set of permutations on {1,2,…,n}. The cut off parameter determines the ratio of penalization of cardinality errors over localization errors. As p increases, while c remaining fixed, OSPA metric gives more penalties to the estimations that are away from all targets of the ground truth [47].

The cut-off parameter was set to 100, and the order was chosen as 1 in the OSPA metric. The labeling error value represents the penalty assigned when mis-associations occur between targets and tracks, and it was also determined as 100. The case study was conducted with the mentioned specifications. The results are given in the following section.

4. Results and Discussion

The results of the case study were divided into two parts. Firstly, the ground truth states, and estimated positions of the targets were compared for the evaluation of accuracy of the algorithms. This analysis aimed to assess how well the radar system was able to track and estimate the positions of the targets. Errors in tracking and association were detailed through OSPA metric, known for its common usage in similar studies.

Secondly, for complexity evaluation, the algorithms were executed 100 times for the same scenario, and their mean computational times were calculated and recorded. This assessment aims to understand the computational requirements of each algorithm and compare their performance in terms of time consumption. While there are studies on reduction of computational complexity, in this paper only the comparison among the three algorithms were done [49].

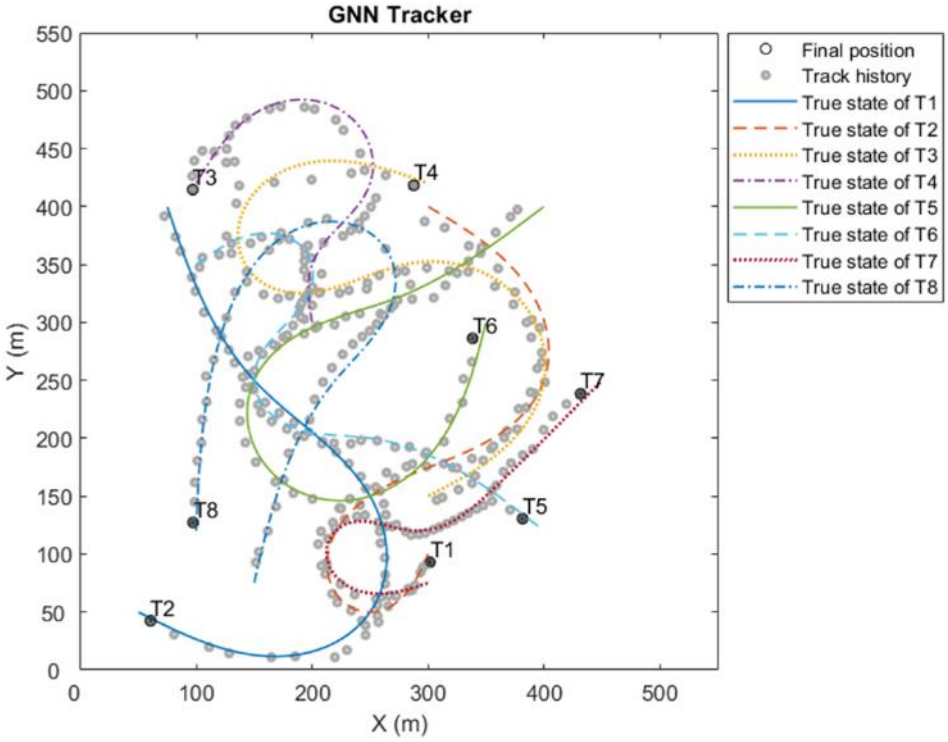

Figure 4. True States (colored lines) and Estimated Tracks (gray circles) with GNN Tracker

Figure 4, Figure 5, and Figure 6 illustrate the tracking results of GNN, JPDA and MHT algorithms with 8 targets, respectively, in x-y coordinates. The same motion scenario was used for all the algorithms for fair comparison. The proximity conditions can be seen on the figures. The colored lines represent true states of the targets and gray circles show track estimation results. The final estimated positions of the targets are denoted by black circles with their corresponding labels (T1, T2, etc.).

40 measurements were done in the scenario. 550 m length of x-axis and y-axis were sufficient to show the trajectories of targets. Motion types of the targets included maneuvering and partially linear motions. In all cases, MTT algorithms operated together with EKF and IMM filters.

In Figure 4, when compared to the other two figures, GNN algorithm has several labeling errors. T1 and T2, T3 and T4, T5 and T6 are mis-associated mutually. JPDA tracker and MHT trackers have no error on labeling.

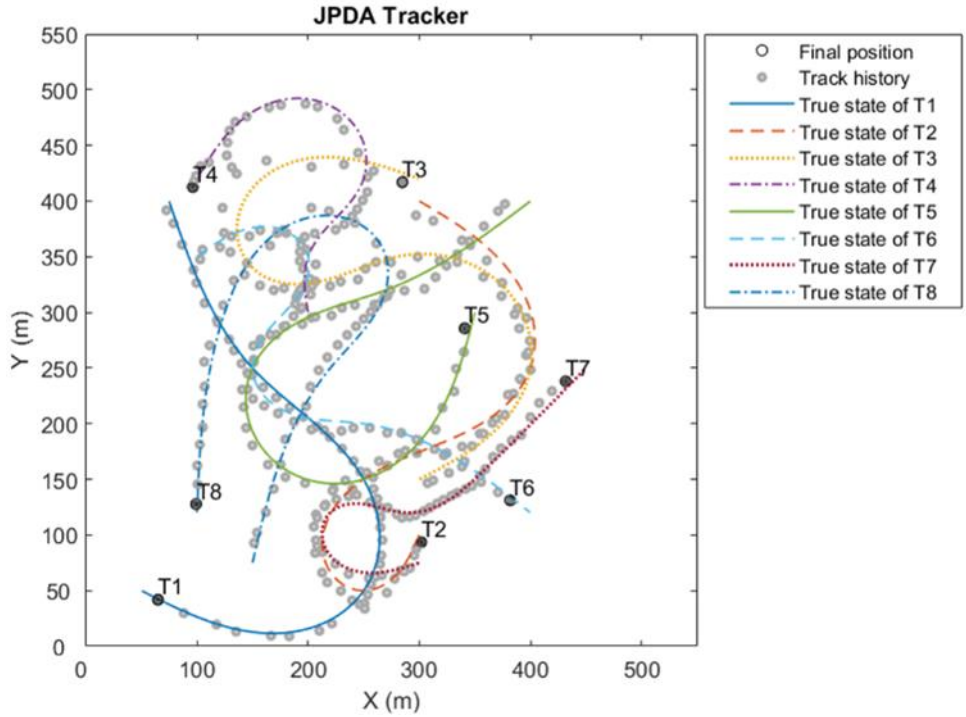

Figure 5. True States and Estimated Tracks with JPDA Tracker

MHT algorithm showed some performance on tracks of T5 and T6 at last steps without losing track of them as depicted in Figure 6. Nevertheless, MHT algorithm managed to distinguish the tracks of T5 and T6. The coalescence effect is a phenomenon where multiple targets are erroneously merged into a single track by a tracking algorithm. This phenomenon occurs when the algorithm incorrectly associates measurements from multiple targets as coming from a single target, leading to the loss of individual target identities [50, 51].

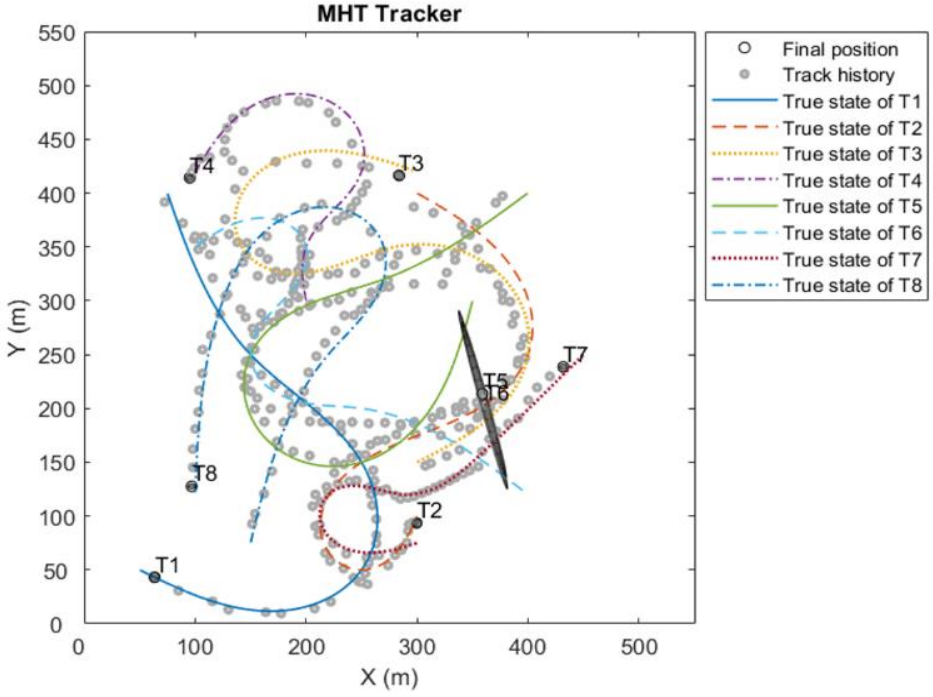

Figure 6. True States and Estimated Tracks with MHT Tracker

OSPA distance results of order p=1 and cut off c=100 for every target were calculated and given in Figure 7, Figure 8, and Figure 9, respectively for GNN, JPDA and MHT algorithms. The graphs are estimation step vs OSPA distance. The labeling error penalty was chosen as 100 not to go higher values and lose details of small values in the graphs.

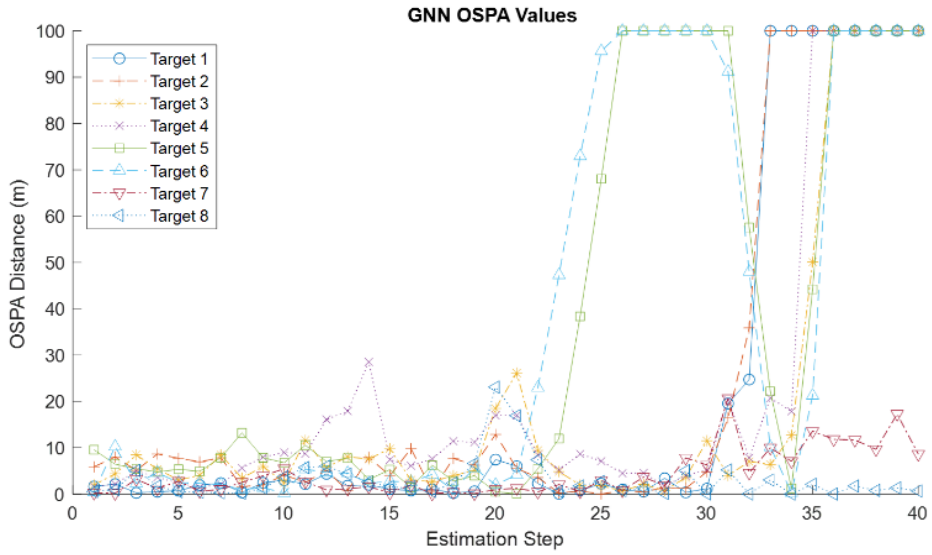

Figure 7. OSPA Position and Labeling Errors of GNN Tracker

In Figure 7, GNN algorithm's bad performance with respect to target labeling is seen. T1 and T2 are mis-labeled starting from 33rd step. T3 and T4 are mis-labeled starting from 35th step. T5 and T6 are mis-labeled at around 25th step but, interestingly, after some steps their OSPA distance again decreases to small values, and then they are mis-labeled again during last 5 steps. Thus, for crucial applications like defense systems, GNN is not appropriate if there is a possibility of close proximity or target cluster conditions.

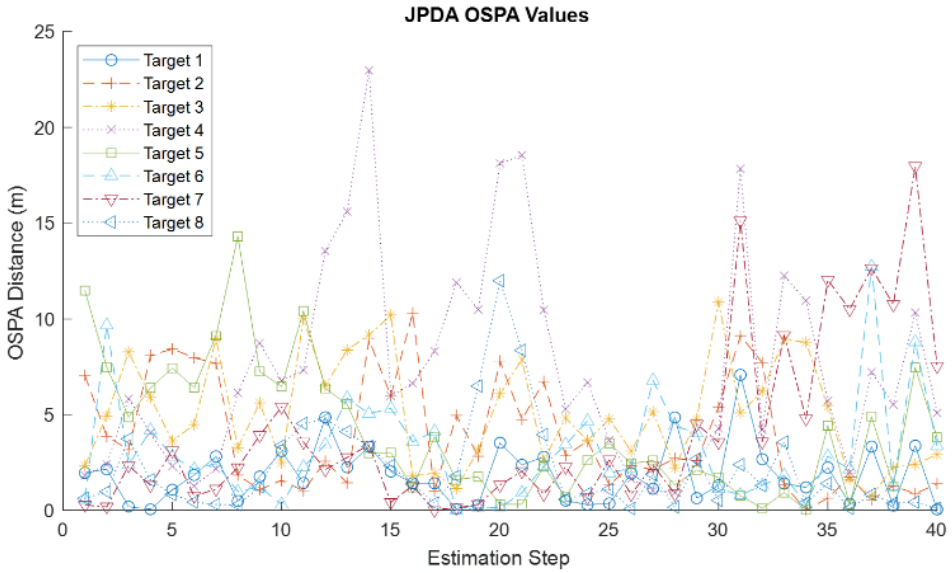

Figure 8. OSPA Position and Labeling Errors of JPDA Tracker

JPDA OSPA distance values shown in Figure 8 seem to be similar to GNN distance values till step 22. Starting from step 22, JPDA values becomes prominent with respect to having good performance, i.e., having smaller OSPA distance values. Even before step 22, the maximum OSPA distance of JPDA algorithm is around 23 m whereas GNN's maximum is around 30 m. MHT algorithm has also the maximum OSPA distance more than 30 m as seen in Figure 9. Thus, JPDA has the best performance looking at the maxima of three graphs. Also, JPDA has only 1 point which has higher than 20 m of OSPA

distance, whereas MHT has 3 targets states as shown in Figure 9, and GNN has 4 OSPA values higher than 20 m, looking at only first 22 steps in Figure 7.

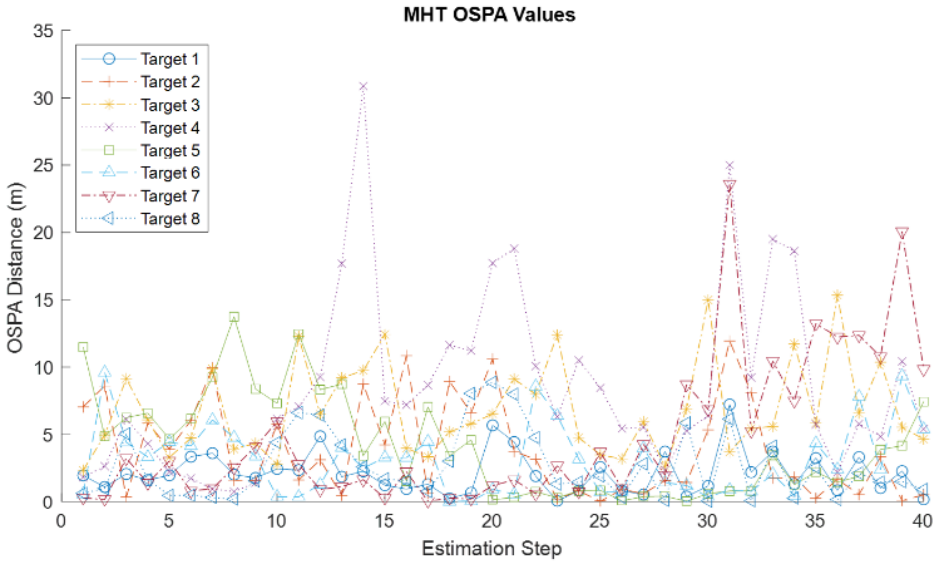

Figure 9. OSPA Position and Labeling Errors of MHT Tracker

In all OSPA graphs, the maximum distance values, excluding mis-labeling cases, occur on T4 at 14th step. The main reason may be that T4 has a linear motion till 13th step, but the motion type changes from linear to maneuvering starting from 13th step. Due to this change, the used filters have additional difficulty on adapting the trajectory of T4, and the MTT algorithms reaches maximum value of OSPA distance at 14th step, i.e., some level of decrease occurs in performance of all algorithms.

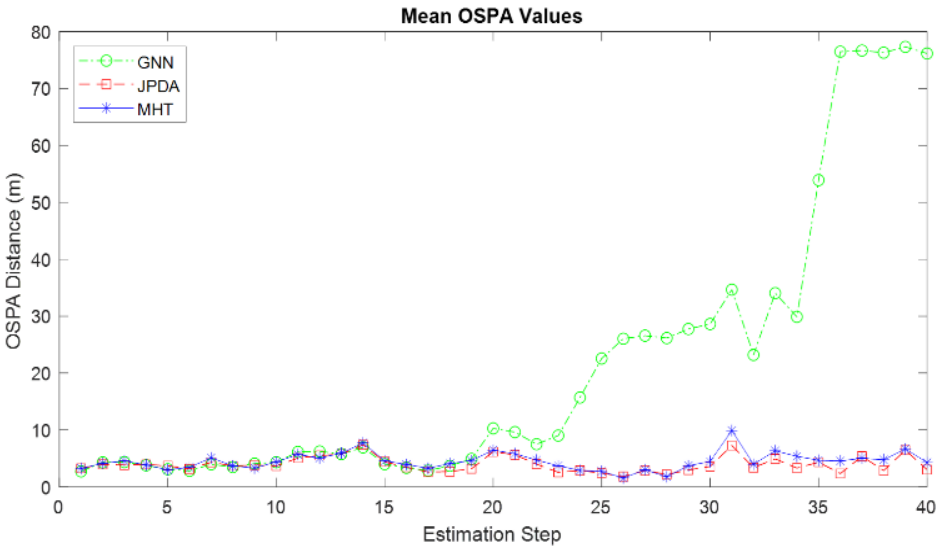

Figure 10. Mean OSPA Errors of the MTT Algorithms

Maxima of OSPA error graphs may not be sufficient to decide about the general performances of the algorithms. It is also necessary to look at their mean OSPA distance values which are depicted in Figure 10. During the first half of the graph in the figure, there is not an important difference among the three algorithms. On the other hand, in the second half, GNN algorithm's high OSPA error values based on labeling mistakes are obviously seen. It reaches 30 m after 25th step whereas JPDA and MHT remains less than 5. After 35th step, GNN algorithm confuses 6 out of 8 targets and it reaches almost 80 m of OSPA distance, noting that the maximum distance value is 100 as stated previously.

Whereas the worst algorithm in accuracy can be decided easily from Figure 10, deciding for the best one with respect to OSPA distances is not easy because JPDA and MHT have near small values to each other. It seems that during the steps 16 to 19, 29 to 36, and 38 JPDA has better performance than MHT.

Table 2. Mean OSPA Error Values and Complexity

Parameter Name	GNN	JPDA	MHT
Mean OSPA distance (m)	21.2	4.2	4.6
Mean computational time (s)	10.1	8.8	31.9

When deciding the best among the three considered algorithms for MTT applications with close proximity, complexity is another important parameter to consider along with performance [52]. Thus, complexity values are also measured and provided in Table 2. They are indicated by mean computational time values which are the averages of running each algorithm 100 times. The processor used in the simulation run is Intel Core i7-6700HQ CPU @ 2.60GHz with 16 GB RAM.

Whereas the mean OSPA distance values of JPDA and MHT are very near to each other in Table 2, GNN's mean distance is around five times the other two with the value 21.2, as expected due to mis-labeling. Therefore, the GNN algorithm can be accepted as the worst algorithm among three. On the other hand, mean computational time values of GNN and JPDA are near to each other as being 10.1 and 8.8, whereas MHT has a much higher value of 31.9 sec. Thus, MHT becomes the worst with respect to computational complexity. As a result, JPDA algorithm is the best algorithm for MTT applications with maneuvering targets in proximity when the two criteria (performance and computational complexity) are considered together.

5. Conclusion

A universal platform for modeling and analysis of end-to-end MTT radar systems together with a comparison of three MTT algorithms on the scenario consisting of maneuvering targets in close proximity was proposed in this paper.

The platform consists of six main sub-blocks which are waveform generation, transmitter, environment and targets, receiver, signal processing, and multitarget tracking. It allows for the modeling and analysis of all aspects of a radar system that affect performance within a single integrated environment. It also enables the analysis and optimization of radar system sub-blocks, including their interdependency and facilitates the study of a wide range of what-if analyses. Additionally, it may be preferred due to its use of more naturally generated data rather than artificial data generation.

On the proposed platform, a case study for MTT of maneuvering targets in close proximity was conducted together with a performance comparison of GNN, JPDA and MHT algorithms. Based on the performance and the computational complexity criteria, the results suggest that the JPDA algorithm is the best choice among the three studied algorithms for MTT of maneuvering targets with proximity.

Author Contributions: Author contributions are as follows: "Conceptualization, M.L.C. and A.E.; methodology, M.L.C. and A.E.; software, M.L.C.; validation, M.L.C. and A.E.; formal analysis, M.L.C. and A.E.; investigation, M.L.C. and A.E.; resources, M.L.C.; data curation, M.L.C. and A.E.; writing—original draft preparation, M.L.C.; writing—review and editing, A.E.; visualization, M.L.C. and A.E.; supervision, A.E. All authors have read and agreed to the published version of the manuscript.

Funding: This research received no external funding.

Data Availability Statement: The data and codes presented in this study are available on request from the corresponding author.

Conflicts of Interest: The authors declare no conflicts of interest.

References

1. M. Guarnieri, "The early history of radar," in IEEE Industrial Electronics Magazine, Sep. 2010. doi: 10.1109/MIE.2010.937936.

2. T. K. Sarkar and M. Salazar Palma, "A history of the evolution of RADAR," in European Microwave Week 2014: Connecting the Future, EuMW 2014 - Conference Proceedings; EuMC 2014: 44th European Microwave Conference, Institute of Electrical and Electronics Engineers Inc., Dec. 2014, pp. 734–737. doi: 10.1109/EuMC.2014.6986539.

3. X. Li, Y. Han, Z. Wang, T. Zhang, Y. Yang, and L. Kong, "Fast antenna de-ployment method for multistatic radar with multiple dynamic surveillance regions," Signal Processing, vol. 170, May 2020, doi: 10.1016/j.sigpro.2019.107419.

4. X. Lu, W. Yi, and Y. Wang, "Adaptive Beam Burden Management for Mul-ti-target Tracking in Distributed Radar Network," Signal Processing, p. 108667, Nov. 2022, doi: 10.1016/j.sigpro.2022.108667.

5. C. Shi, Y. Wang, F. Wang, S. Salous, and J. Zhou, "Power resource allocation scheme for distributed MIMO dual-function radar-communication system based on low probability of intercept," Digital Signal Processing: A Review Journal, vol. 106, Nov. 2020, doi: 10.1016/j.dsp.2020.102850.

6. K. Zhong, J. Hu, C. Pan, X. Yu, and X. Li, "MIMO Radar Beampattern Design Based on Manifold Optimization Method," IEEE Communications Letters, vol. 26, no. 5, pp. 1086–1090, May 2022, doi: 10.1109/LCOMM.2022.3149909.

7. J. Kannanthara, D. Griffiths, M. Jahangir, J. M. Jones, C. J. Baker, M. Anto-niou, ... & Y. Singh, "Whole system radar modelling: Simulation and validation," IET Radar, Sonar & Navigation, vol. 17, pp. 1050-1060, 2023, doi: 10.1049/rsn2.12399

8. M. Beard, B. T. Vo, and B. N. Vo, "A Solution for Large-Scale Multi-Object Tracking," IEEE Transactions on Signal Processing, vol. 68, pp. 2754–2769, 2020, doi: 10.1109/TSP.2020.2986136.

9. Z. X. Liu, J. Gan, J. S. Li, and M. Wu, "Adaptive δ-Generalized Labeled Mul-ti-Bernoulli Filter for Multi-Object Detection and Tracking," IEEE Access, vol. 9, pp. 2100–2109, 2021, doi: 10.1109/ACCESS.2020.3047802.

10. P. Gu, Z. Jing, and L. Wu, "A novel adaptive δ-generalised labelled mul-ti-Bernoulli filter for multi-target tracking with heavy-tailed noise," IET Radar, Sonar and Navigation, Mar. 2022, doi: 10.1049/rsn2.12351.

11. F. Goodall and B. I. A. Aveillant, "Adaptation of Multi-target Tracker Using Neural Networks in Drone Surveillance Radar," in 2023 IEEE Radar Conference (Ra-darConf23), IEEE, May 2023, pp. 1–6.

12. L. Ding, C. Shi, and J. Zhou, "Collaborative route optimization and resource management strategy for multi-target tracking in airborne radar system," Digital Sig-nal Processing: A Review Journal, vol. 138, Jun. 2023, doi: 10.1016/j.dsp.2023.104051.

13. J. Luo, Y. Han, and L. Fan, "Underwater acoustic target tracking: A review," Sensors (Switzerland), vol. 18, no. 1. MDPI AG, Jan. 02, 2018. doi: 10.3390/s18010112.

14. S. Kamkar, F. Ghezloo, H. A. Moghaddam, A. Borji, and R. Lashgari, "Mul-tiple-target tracking in human and machine vision," PLoS Computational Biology, vol. 16, no. 4. Public Library of Science, Apr. 01, 2020. doi: 10.1371/journal.pcbi.1007698.

15. C. Gouveia, J. Vieira, and P. Pinho, "A review on methods for random mo-tion detection and compensation in bio-radar systems," Sensors (Switzerland), vol. 19, no. 3. MDPI AG, Feb. 01, 2019. doi: 10.3390/s19030604.

16. B. Bati and N. Duru, "Maritime automatic target recognition for ground-based scanning radars by using sequential range profiles," Turkish Journal of Electrical Engineering and Computer Sciences, vol. 29, no. 2, pp. 929–943, 2021, doi: 10.3906/ELK-2004-143.

17. E. Ho, A. Rajagopalan, A. Skvortsov, S. Arulampalam, and M. Piraveenan, "Game Theory in Defence Applications: A Review," Sensors, vol. 22, no. 3. MDPI, Feb. 01, 2022. doi: 10.3390/s22031032.

18. L. Rakai, H. Song, S. J. Sun, W. Zhang, and Y. Yang, "Data association in multiple object tracking: A survey of recent techniques," Expert Systems with Applica-tions, vol. 192. Elsevier Ltd, Apr. 15, 2022. doi: 10.1016/j.eswa.2021.116300.

19. S. Liu, H. Pan, L. Xiao, and B. Zhang, "Multi-hypothesis Data Association for Multiple Target Tracking," in IEEE Conference on Telecommunications, Optics and Computer Science (TOCS), Institute of Electrical and Electronics Engineers (IEEE), Jan. 2022, pp. 231–236. doi: 10.1109/tocs56154.2022.10016172.

20. Y. Bar-Shalom, T. E. Fortmann, and P. G. Cable, "Tracking and Data Asso-ciation," J Acoust Soc Am, vol. 87, no. 2, pp. 918–919, Feb. 1990, doi: 10.1121/1.398863.

21. J. Liu, L. Bai, Y. Xia, T. Huang, and B. Zhu, "GNN-PMB: A Simple but Effec-tive Online 3D Multi-Object Tracker without Bells and Whistles," IEEE Transactions on Intelligent Vehicles, Feb. 2022, doi: 10.1109/TIV.2022.3217490.

22. M. K. Kalandros, L. Trailovic, L. Y. Pao, and Y. Bar-Shalom, "Tutorial on multisensor management and fusion algorithms for target tracking," Institute of Elec-trical and Electronics Engineers (IEEE), May 2004, pp. 4734–4748 vol.5. doi: 10.23919/acc.2004.1384060.

23. J. Vermaak, S. J. Godsill, and P. Pérez, "Monte Carlo filtering for mul-ti-target tracking and data association," IEEE Trans Aerosp Electron Syst, vol. 41, no. 1, pp. 309–332, Jan. 2005, doi: 10.1109/TAES.2005.1413764.

24. D. B. Reid, "An Algorithm for Tracking Multiple Targets," IEEE Trans Au-tomat Contr, vol. 24, no. 6, pp. 843–854, 1979, doi: 10.1109/TAC.1979.1102177.

25. C. Kim, F. Li, A. Ciptadi, and J. M. Rehg, "Multiple Hypothesis Tracking Re-visited," 2015.

26. L. S. Jong, "Reducing hypotheses in MHT when everything might, but nothing happens," Thesis, Eindhoven University of Technology, Eindhoven, 2021. [Online]. Available: http://www.tue.nl/en/university/about-the-university/integrity/scientific-integrity/

27. J. Park and C. G. Park, "Multi-target Tracking Based on Gaussian Mixture Labeled Multi-Bernoulli Filter with Adaptive Gating," Seoul: First International Sym-posium on Instrumentation, Control, Artificial Intelligence, and Robotics (ICA-SYMP), 2019.

28. J. Smith, F. Particke, M. Hiller, and J. Thielecke, "Systematic Analysis of the PMBM, PHD, JPDA and GNN Multi-Target Tracking Filters," in 22nd International Conference on Information Fusion, Ottawa, Canada: International Society of Infor-mation Fusion, Jun. 2019.

29. C. Qu, Y. Zhang, X. Zhang, and Y. Yang, "Reinforcement learning-based data association for multiple target tracking in clutter," Sensors (Switzerland), vol. 20, no. 22, pp. 1–29, Nov. 2020, doi: 10.3390/s20226595.

30. P. K. Sharma, "Data association algorithms for multi target tracking in a probabilistic framework,", M.S. thesis, Eindhoven University of Technology, Eindho-ven, 2021.

31. B. R. Mahafza, "Radar Systems Analysis and Design Using Matlab", 3rd Edition. Alabama, USA: CRC Press, 2013.

32. J. S. Patel, F. Fioranelli, and D. Anderson, "Review of radar classification and RCS characterisation techniques for small UAVs or drones," IET Radar, Sonar and Navigation, vol. 12, no. 9. Institution of Engineering and Technology, pp. 911–919, Sep. 01, 2018. doi: 10.1049/iet-rsn.2018.0020.

33. V. Semkin et al., "Analyzing Radar Cross Section Signatures of Diverse Drone Models at mmWave Frequencies," IEEE Access, vol. 8, pp. 48958–48969, 2020, doi: 10.1109/ACCESS.2020.2979339.

34. T. Thomas and S. Sreeja, "Comparison of Nearest Neighbor and Probabilis-tic Data Association Filters for Target Tracking in Cluttered Environment," in 2021 IEEE 6th International Conference on Computing, Communication and Automation, ICCCA 2021, Institute of Electrical and Electronics Engineers Inc., 2021, pp. 272–277. doi: 10.1109/ICCCA52192.2021.9666392.

35. S. He, H. S. Shin, and A. Tsourdos, "Trajectory optimization for multitarget tracking using joint probabilistic data association filter," Journal of Guidance, Control, and Dynamics, vol. 43, no. 1, pp. 170–178, 2020, doi: 10.2514/1.G004249.

36. Q. Li, R. Li, K. Ji, and W. Dai, "Kalman filter and its application," in Pro-ceedings - 8th International Conference on Intelligent Networks and Intelligent Sys-tems, ICINIS 2015, Institute of Electrical and Electronics Engineers Inc., Aug. 2016, pp. 74–77. doi: 10.1109/ICINIS.2015.35.

37. M. Khodarahmi and V. Maihami, "A Review on Kalman Filter Models," Archives of Computational Methods in Engineering, vol. 30, no. 1. Springer Science and Business Media B.V., pp. 727–747, Jan. 01, 2023. doi: 10.1007/s11831-022-09815-7.

38. G. Hakobyan and B. Yang, "High-Performance Automotive Radar: A re-view of signal processing algorithms and modulation schemes," IEEE Signal Process Mag, vol. 36, no. 5, pp. 32–44, Sep. 2019, doi: 10.1109/MSP.2019.2911722.

39. S. Arumugam, S. Manoharan, V. Bhaskar, and P. Sandeep Kumar, "A Com-prehensive Review on Automotive Antennas for Short Range Radar Communications," Wirel Pers Commun, vol. 127, no. 3, pp. 2667–2694, Dec. 2022, doi: 10.1007/s11277-022-09890-w.

40. S. H. Javadi and A. Farina, "Radar networks: A review of features and challenges," Information Fusion, vol. 61, pp. 48–55, Sep. 2020, doi: 10.1016/j.inffus.2020.03.005.

41. A. Guerra, D. Dardari, and P. M. Djuric, "Dynamic Radar Networks of UAVs: A Tutorial Overview and Tracking Performance Comparison with Terrestrial Radar Networks," IEEE Vehicular Technology Magazine, vol. 15, no. 2, pp. 113–120, Jun. 2020, doi: 10.1109/MVT.2020.2979698.

42. M. Jankiraman, FMCW Radar Design. Artech House, 2018.

43. M. A. Richards, "Fundamentals of Radar Signal Processing, Second Edition (McGraw-Hill Professional Engineering)," 2014.

44. "https://www.miwv.com/standard-gain-horn-antennas/," Millimeter Wave Products Inc.

45. S. Li, M. Cui, L. Szilagyi, C. Carta, and F. Ellinger, "A 79 GHz reconfigurable highly linear Low-Noise Amplifier for Civil-Automotive Short-Range-Radars in 22-nm FD-SOI CMOS," in 2022 17th European Microwave Integrated Circuits Conference, EuMIC 2022, Institute of Electrical and Electronics Engineers Inc., 2022, pp. 248–251. doi: 10.23919/EuMIC54520.2022.9922964.

46. B. Ristic, B. N. Vo, D. Clark, and B. T. Vo, "A metric for performance evaluation of multi-target tracking algorithms," IEEE Transactions on Signal Processing, vol. 59, no. 7, pp. 3452–3457, Jul. 2011, doi: 10.1109/TSP.2011.2140111.

47. D. Schuhmacher, B. T. Vo, and B. N. Vo, "A consistent metric for performance evaluation of multi-object filters," IEEE Transactions on Signal Processing, vol. 56, no. 8 I, pp. 3447–3457, Aug. 2008, doi: 10.1109/TSP.2008.920469.

48. Y. Song, Z. Hu, T. Li, and H. Fan, "Performance Evaluation Metrics and Approaches for Target Tracking: A Survey," Sensors, vol. 22, no. 3. MDPI, Feb. 01, 2022. doi: 10.3390/s22030793.

49. M. L. Cobankaya and A. B. Elrouby. "Sectoring Approach for Performance Enhancement of MTT and Its Application on JPDA Algorithm.", IEEE Access, April 2025, doi: 10.1109/ACCESS.2025.3560601.

50. R. D. Palkki, A. D. Lanterman, and W. D. Blair, "Addressing Track Hypothesis Coalescence in Sequential K-Best Multiple Hypothesis Tracking," IEEE Transactions on Aerospace and Electronic System, 2011.

51. T. Kropfreiter, F. Meyer, S. Coraluppi, C. Carthel, R. Mendrzik, and P. Willett, "Track Coalescence and Repulsion: MHT, JPDA, and BP," in IEEE 24th International Conference on Information Fusion (FUSION), IEEE, Sep. 2021. [Online]. Available: http://arxiv.org/abs/2109.01523

52. Z. Wei, Z. Duan, Y. Han, and M. Mallick, "A New Coarse Gating Strategy Driven Multidimensional Assignment for Two-Stage MHT of Bearings-Only Multisen-sor-Multitarget Tracking," Sensors, vol. 22, no. 5, Mar. 2022, doi: 10.3390/s22051802.